School of Mathematical
and Physical Sciences

University of Reading

Department of Mathematics and Statistics

Preprint MPS-2012-07

01 March 2012

On Discrimination Algorithms for Ill-Posed Problems with an Application to Magnetic Tomography

by

Natalie Lowery, Roland Potthast, Maria Vahdati and William Holderbaum

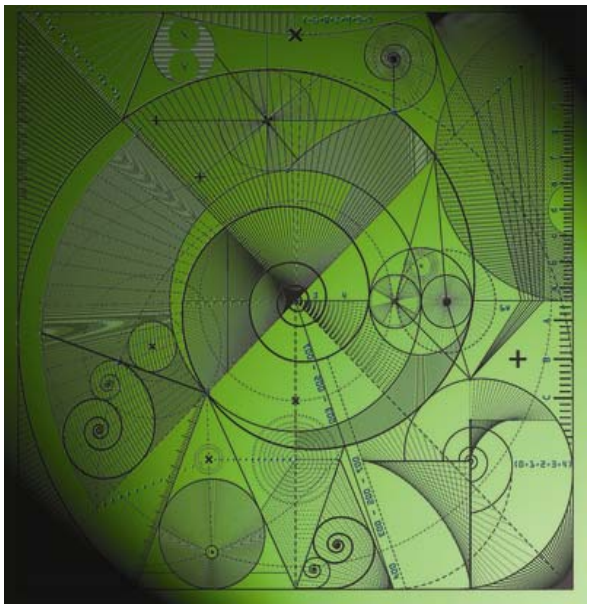

On Discrimination Algorithms for Ill-Posed Problems with an Application to Magnetic Tomography

Natalie Lowery [1,2], Roland Potthast[1], Maria Vahdati[2] and William Holderbaum[3]

[1] Department of Mathematics, University of Reading, Whiteknights, PO Box 220, Berkshire RG6 6AX, UK

[2] Department of Construction Management, University of Reading, Whiteknights, PO Box 220, Berkshire RG6 6AX, UK

[3] Department of Systems Engineering, University of Reading, Whiteknights, PO Box 220, Berkshire RG6 6AX, UK

E-mail: n.l.h.lowery@student.reading.ac.uk, r.w.e.potthast@reading.ac.uk, m.m.vahdati@reading.ac.uk and w.holderbaum@reading.ac.uk

Abstract.

In this paper we explore classification techniques for ill-posed problems. Two classes are *linearly separable* in some Hilbert space X if they can be separated by a hyperplane. We investigate *stable separability*, i.e. the case where we have a positive distance between two separating hyperplanes. When the data in the space Y is generated by a compact operator A applied to the system states $\varphi \in X$, we will show that in general we do not obtain stable separability in Y even if the problem in X is stably separable. In particular, we show this for the case where a nonlinear classification is generated from a non-convergent family of linear classes in X.

We apply our results to the problem of quality control of fuel cells where we classify fuel cells according to their efficiency. We can potentially classify a fuel cell using either some external measured magnetic field or some internal current. However we cannot measure the current directly since we cannot access the fuel cell in operation. The *first* possibility is to apply discrimination techniques directly to the measured magnetic fields. The *second* approach first reconstructs currents and then carries out the classification on the current distributions. We show that both approaches need regularization and that the regularized classifications are not equivalent in general.

Finally, we investigate a widely used linear classification algorithm *Fisher's linear discriminant* with respect to it's ill-posedness when applied to data generated via a compact integral operator. We show that the method cannot stay stable when the number of measurement points becomes large.

1. Introduction

Classification techniques have been applied widely in medical imaging, process monitoring and computer science, for example to face recognition [10] and classification

of tumours [1]. In [4] the cancer area classification problem is investigated with voxels produced by (DCE-)MRI data as inputs. The author uses unsupervised clustering techniques first and then goes on to classify the voxels in the tumoral regions where 'voxels of the same cluster are fed with the same label into the classifier'. The magnetic tomography problem which we will investigate as our main application appears in the form of MEG in medical problems; and it is an important tool for quality control in fuel cell engineering.

Many medical imaging or reconstruction techniques are instable or *ill-posed* with respect to the measurements and a variety of regularization methods to treat this instability have been introduced in recent years ([8], [6], [15], [20]). The phenomenon is much less studied for classification methods, though the classification method usually inherits the underlying ill-posedness from the operator which generates the data under consideration.

A problem is called ill-posed according to Hadamard (compare [6]), if the solution does not always exist, if it is non-unique or does not depend stably on the measured data. For example, a classification problem often is ill-posed when there is a small amount of input data but the dimensionality of the input data is relatively large. This can be dealt with in a number of different ways. In [5] a semi-supervised learning approach is considered whereby both labelled and unlabelled data is used in training. Regularization methods are often used to give an approximate solution of an ill-posed problem. For example for the problem of cancer classification and the inverse problem of computational vision [1] and [19] respectively use regularization methods to restore stability. In [7] the authors discuss several discrimination methods that can be used for the problem of cancer classification including Fisher's linear discriminant. Fisher's linear discriminant is found to perform poorly here, since 'the matrices of between-group and within-group sums of squares and cross-products are quite unstable' [7]. For our problem classification via magnetic field yields an unstable within-class scatter matrix too, which we deal with by using regularization techniques.

The key purpose of this work is threefold. *First*, we want to investigate the phenomenon of ill-posedness of supervised classification algorithms in a rather general framework by looking at separating hyperplanes in a Hilbert space setting. We will show that with a compact operator $A : X \to Y$ generating the data $y^{(\omega)} \in Y$ with some index $\omega \in \Xi$, in general the classification problem applied to data $y^{(\omega)} = A\varphi^{(\omega)} \in Y$ is unstable, even if the original system states $\varphi^{(\omega)} \in X$ can be stably separated. We will study several key situations in which the different phenomena can be clearly observed, for example a case where classes are defined by the singular vectors of the operator A. An important observation will be that stable separation in the image space under an operator A depends on the condition $v \in A^*Y$ for the normal vector v to the hyperplane in the state space.

Second, we investigate a popular classification method, *Fisher's Linear Discriminant*, with respect to it's ill-posedness, when the dimensionality of the space of

training patterns which are used for discrimination is high. We show that, in the case of data generated by a compact integral operator, it cannot stay stable when the number of measurement points tends to infinity.

Third, we investigate the application of classification algorithms to classify *fuel cells* according to their efficiency. Fuel cells work by electrolysis, compare [3] for more details. An issue is that fuel cells can be unreliable [18] and it is difficult to determine their efficiency since, unlike a standard engine, they do not have moving parts [12]. This makes quality control of fuel cells extremely difficult in both their manufacture and maintainance.

We can potentially classify a fuel cell by its *current* or by its *magnetic field*. However if we wish to classify a fuel cell by its current, we must first use techniques in magnetic tomography to reconstruct the current from the magnetic field as introduced in [17], [22]. The second option carries out a classification without performing any reconstruction of the current of the current densities. This is carried out by an application of linear classification techniques. We will see that the classification of fuel cells by their magnetic field is instable in general. Also, we provide a regularization for the classification and investigate the relation of a regularized classification via the magnetic field with the classification by the regularized reconstruction of the current densities. We show that the two approaches are not equivalent in general.

The structure of the subsequent sections is as follows. First, we investigate linear and particular nonlinear supervised classification techniques in Section 2. In Section 3 we summarize the results of static magnetic tomography. We focus on the ill-posedness of the problem and describe discrete versions of the magnetic field and current operators involved. The ill-posedness of classification problems for magnetic tomography is investigated in Section 4. We then study the ill-posedness of Fisher's Linear Discriminant applied to data generated by a compact operator in Section 5. Here, we also show that regularization applied to the classification generally is not identical to the classification applied to a regularized solution. Finally, we provide numerical examples from magnetic tomography in Section 5.3.

2. Classification and Ill-Posedness

Here, we will think of classification as a tool to define or identify a subset C of some space X. We will restrict our attention to Hilbert spaces X with some scalar product $\langle \cdot, \cdot \rangle$. All elements in C are considered as elements of class C. If C is an affine halfspace, U in X, then we call the classification *linear*, i.e. if C is given in the form

$$U := \{x : \ \langle x, v \rangle \geq \rho\} \tag{2.1}$$

with some vector $v \in X$ and a number $\rho \in \mathbb{R}$. A linear class is uniquely described by a vector v with $||v|| = 1$ and the number ρ. The number ρ gives the distance of the boundary of the halfspace to the origin of X and is called *affine distance*. We will also

study particular nonlinear classes which are obtained from linear classes as intersections of affine halfspaces U_ℓ, $\ell = 1, ..., n$, i.e.

$$C := \bigcap_{l=1}^{n} U_\ell. \tag{2.2}$$

In this case we can reduce the study of stability of the classification to the stability in the linear case. For smooth classes, i.e. where the boundary of C is a smooth manifold in X, we can locally approximate the general nonlinear classification by a linear classification, such that in this case the stability analysis can also be carried over from the linear to the nonlinear case.

The process of classification is given by the way to achieve a definition of a class C.

Definition 2.1 (Supervised Classification) *Classification methods start with some elements or* samples $x_1^{(1)}, ..., x_1^{(N_1)} \in X$*, also known as a training set. The task here is to define an appropriate set* $C_1 \subset X$ *such that all elements* $x_1^{(\omega)}$, $\omega = 1, ..., N_1$ *are in* C_1*. Often, there are also elements* $x_2^{(\omega)}$, $\omega = 1, ..., N_2$ *of a complementary class* $C_2 = X \setminus C_1$*. We may also have access to some* target values *which indicate which class these samples belong to. We call an algorithm a* supervised classification algorithm*, if it takes the samples and corresponding target values as input and calculates the classes* C_1*,* C_2 *in such a way that new samples can be classified successfully.*

Before we consider a particular classification algorithm, we first study the behaviour of a class C and its image $\tilde{C} = AC$ with some linear operator A in a general framework. We will put a particular emphasis on classes which are composed of a set of linear classes.

2.1. General Results on the Ill-Posedness of Classification in the Image Space

Here, we investigate classification in connection with ill-posed problems. We assume that we have Hilbert spaces X, Y with scalar products $\langle \cdot, \cdot \rangle$ and a compact linear operator $A : X \to Y$. We are interested in supervised classification problems and their interplay with the instability of the inverse A^{-1} of A.

To be more precise, let us assume that we have two Classes C_1, C_2 in X which are linearly separable, i.e. we assume that there is halfspace $U_1 \subset X$ which contains C_1 and has no intersection with C_2. We are interested in the stability of the separation. We call two classes stably separable, if there are two halfspaces U_1, U_2 with positive distance $\rho > 0$ such that $C_1 \subset U_1$ and $C_2 \subset U_2$. In this case, if we have measurements of elements $x_1 \in C_1$ or $x_2 \in C_2$ with error of size smaller than $\rho/2$, then we can still identify x_1 as an element of C_1 and x_2 as an element of C_2.

Compact operators $A : X \to Y$ have the property that the image of a bounded sequence has a convergent subsequence. In general, there can be elements x_1, x_2 in X which are well separated, i.e. $||x_1 - x_2|| \geq \rho$, but the distance $||y_1 - y_2||$ of the images $y_\xi := Ax_\xi$, $\xi = 1, 2$, is arbitrarily small. Here, our goal is to investigate the situation

when we study stable classifications in X and how they can be achieved on the images in Y without the inversion of the operator A.

A generic example. As a first step towards the clarification of the situation we first want to consider a special case. We use the singular value decomposition of the operator A, compare [6], i.e. we have an orthonormal basis $\{\varphi_\ell \in X, \ \ell \in \mathbb{N}\}$ in X and an orthonormal basis $\{g_\ell \in Y, \ \ell \in \mathbb{N}\}$ and a monotonously decreasing sequence $(\mu_\ell)_{\ell\in\mathbb{N}}$ of positive real values such that

$$A\varphi_\ell = \mu_\ell g_\ell, \ \ A^* g_\ell = \mu_\ell \varphi_\ell \tag{2.3}$$

for all $\ell \in \mathbb{N}$. We define a linear stable classification by

$$C^{(1)}_{\ell,\rho} := \{x : \ \langle x, \varphi_\ell\rangle \geq \rho\}, \ \ C^{(2)}_{\ell,\rho} := \{x : \ \langle x, \varphi_\ell\rangle \leq -\rho\}, \tag{2.4}$$

which we call a *stable linear separation along the direction of the singular values*. Clearly, the distance between $C^{(1)}_{\ell,\rho}$ and $C^{(2)}_{\ell,\rho}$ is $2\rho > 0$. For every pair $C^{(1)}_{\ell,\rho}, C^{(2)}_{\ell,\rho}$ from the sequence of classes the classification is stable uniformly with respect to $\ell \in \mathbb{N}$.

The images of the classes $C^{(1)}_{\ell,\rho}, C^{(2)}_{\ell,\rho}$ under the application of the operator A is given by

$$\begin{aligned}
\tilde{C}^{(1)}_{\ell,\rho} &:= \{y = Ax : \ \langle x, \varphi_\ell\rangle \geq \rho\}, \\
&= \{y \in A(X) : \ \langle A^{-1}y, \varphi_\ell\rangle \geq \rho\}, \\
&= \{y \in A(X) : \ \langle y, (A^*)^{-1}\varphi_\ell\rangle \geq \rho\}, \\
&= \left\{y \in A(X) : \ \left\langle y, \tfrac{1}{\mu_\ell} g_\ell \right\rangle \geq \rho\right\}, \\
&= \{y \in A(X) : \ \langle y, g_\ell\rangle \geq \mu_\ell \rho\},
\end{aligned} \tag{2.5}$$

and

$$\tilde{C}^{(2)}_{\ell.\rho} := \{y : \ \langle y, g_\ell\rangle \leq -\mu_\ell \rho\}. \tag{2.6}$$

The distance between the classes $\tilde{C}^{(1)}_{\ell,\rho}$ and $\tilde{C}^{(2)}_{\ell,\rho}$ is $2\mu_\ell\rho$. The distance is depending on $\ell \in \mathbb{N}$ and since the singular values μ_ℓ tend to zero for $\ell \to \infty$, the stability of the separation of the pairs of classes is no longer uniform in ℓ. We summarize these basic but important observations in the following lemma.

LEMMA 2.2 *Consider a compact linear operator A between Hilbert spaces X and Y. Then the image classes for stable linear separation along the direction of the singular values for a uniform separation distance ρ will no longer be uniformly separable in the image space Y.*

The general case. Next, we consider the general case of a sequence of linear classes $C_1, C_2, C_3, ...$ Let v_ℓ, $\ell \in \mathbb{N}$ be the corresponding vectors in X and ρ_ℓ, $\ell \in \mathbb{N}$ be the affine distances. Here, we also assume that the sequence (v_ℓ) does not have a convergent subsequence. Clearly, the classes are given by

$$C_\ell = \{x : \ \langle x, v_\ell\rangle \geq \rho_\ell\}, \ \ \ell \in \mathbb{N}. \tag{2.7}$$

We use a calculation similar to (2.5) to show that if v_ℓ is in the range of A^*, then

$$\tilde{C}_\ell := AC_\ell = \{y : \ \langle y, (A^*)^{-1} v_\ell \rangle \geq \rho_\ell\}. \tag{2.8}$$

With the definition

$$\psi_\ell := (A^*)^{-1} v_l \tag{2.9}$$

we can write this in the form

$$\tilde{C}_\ell := AC_\ell = \left\{y : \ \left\langle y, \tfrac{\psi_\ell}{||\psi_\ell||} \right\rangle \geq \tfrac{\rho_\ell}{||\psi_\ell||} \right\}. \tag{2.10}$$

Here, the distance of the image class boundary to the origin of Y is given by

$$\tilde{\rho}_\ell := \frac{\rho_\ell}{||\psi_\ell||}, \ \ \ell \in \mathbb{N}. \tag{2.11}$$

We are now prepared to prove the following basic instability result.

THEOREM 2.3 *Let C_ℓ, $\ell \in \mathbb{N}$ be linear classes in X with boundary of distance ρ_ℓ to the origin such that $(\rho_\ell)_{\ell \in \mathbb{N}}$ is bounded. We assume that the vectors $v_\ell \in X$ do not contain a convergent subsequence. Further, let $A : X \to Y$ be a compact linear operator such that $v_\ell \in A^*Y$ for $\ell \in \mathbb{N}$. Then for $\tilde{\rho}_\ell$ defined in (2.11) there will be a subsequence ℓ_k, $k \in \mathbb{N}$, of the image classes $\tilde{C}_\ell := AC_\ell$ in Y with*

$$\tilde{\rho}_{\ell_k} \to 0, \ \ k \to \infty. \tag{2.12}$$

Proof. We show that for ψ_ℓ defined in (2.9) there is a subsequence ℓ_k, $k \in \mathbb{N}$, such that

$$||\psi_{\ell_k}|| \to \infty, \ \ k \to \infty. \tag{2.13}$$

Since A is compact, also A^* is a compact operator $Y \to X$. We carry out a proof via contradiction. Assume that the sequence $(\psi_\ell)_{\ell \in \mathbb{N}}$ is bounded in Y. Then, it must contain a weakly convergent subsequence. Since A^* is a compact operator $Y \to X$, in this case the image sequence

$$(v_\ell)_{\ell \in \mathbb{N}} = A^*(\psi_\ell)_{\ell \in \mathbb{N}} \tag{2.14}$$

defined via (2.9) must contain a convergent subsequence. However, we have assumed that this is not the case. Thus, in this case $(\psi_\ell)_{\ell \in \mathbb{N}}$ cannot be bounded in Y, i.e. we have shown (2.13). Since $(\rho_\ell)_{\ell \in \mathbb{N}}$ is bounded, from (2.13) and (2.11) we now finally conclude (2.12). □

For the previous result we needed to impose the condition $v_\ell \in A^*(Y)$ for $\ell \in \mathbb{N}$. To study the case where this condition is no longer satisfied, we need to investigate regularization of classifications.

2.2. Regularization of Classifications.

The image class AC of some class $C = \{x \in X : \langle x, v\rangle \geq \rho\}$ under a compact linear operator $A : X \to Y$ is given by

$$\tilde{C} := AC = \{y \in A(X) : \langle A^{-1}y, v\rangle \geq \rho\}. \tag{2.15}$$

If $v \in A^*(X)$, then this can be transformed into

$$\tilde{C} = \{y \in A(X) : \langle y, (A^*)^{-1}v\rangle \geq \rho\}. \tag{2.16}$$

The operators A^{-1} and $(A^*)^{-1}$ are unbounded and it will be an important step for the analysis of the ill-posedness of classifications in Y to study the regularized version of (2.15). To this end we use $R_\alpha = (\alpha I + A^*A)^{-1}A^*$ to define the *regularized image class*

$$\tilde{C}_\alpha := \{y \in A(X) : \langle R_\alpha y, v\rangle \geq \rho\}. \tag{2.17}$$

If we need to study this class in dependence of ρ, we use the notation $\tilde{C}_\alpha = \tilde{C}_\alpha^{(\rho)}$. We calculate

$$\begin{aligned}\tilde{C}_\alpha &= \{y \in A(X) : \langle R_\alpha y, v\rangle \geq \rho\} \\ &= \{y \in A(X) : \langle y, R_\alpha^* v\rangle \geq \rho\}.\end{aligned} \tag{2.18}$$

We note that

$$\begin{aligned}R_\alpha^* &= \left((\alpha I + A^*A)^{-1}A^*\right)^* \\ &= A(\alpha I + A^*A)^{-1} \\ &= (\alpha I + AA^*)^{-1}A,\end{aligned} \tag{2.19}$$

where the last equality is obtained by multiplication by the invertible operators $\alpha I + A^*A$ from the right and $\alpha I + AA^*$ from the left. Thus, the adjoint of the Tikhonov operator R_α is the Tikhonov operator for the adjoint A^*. Now, if v is in $A^*(Y)$, then we have the convergence

$$R_\alpha^* v \to (A^*)^{-1}v, \quad \alpha \to 0. \tag{2.20}$$

In this case we have

$$\left\langle y, (A^*)^{-1}v\right\rangle = \lim_{\alpha\to 0} \left\langle y, R_\alpha^* v\right\rangle. \tag{2.21}$$

The upcoming arguments basically work as follows. We have a bounded linear form $L(y)$ on Y and a family of bounded linear forms $L_\alpha(y)$ with $L_\alpha(y) \to L(y)$ for $\alpha \to 0$ for every fixed $y \in Y$. Let α_ℓ be a sequence of parameters with $\alpha_\ell \to 0$ for $\ell \to \infty$. Then from $L_{\alpha_\ell}(y) \geq \rho$ for all sufficiently small $\alpha_\ell > 0$, we deduce that $L(y) \geq \rho$. Further, if $L(y) \geq \rho$, we have that for any $\epsilon > 0$ we know that $L_{\alpha_\ell}(y) \geq \rho - \epsilon$ for all sufficiently small α_ℓ. However, for $\epsilon = 0$ this is not the case in general, which makes the following arguments necessary. We obtain that

$$\left\langle y, R_{\alpha_\ell}^* v\right\rangle \geq \rho \; \forall \alpha_\ell > 0 \text{ suff. small} \;\; \Rightarrow \left\langle y, (A^*)^{-1}v\right\rangle \geq \rho. \tag{2.22}$$

and thus

$$y \in \tilde{C}_{\alpha_\ell} \forall \alpha_\ell \text{ suff. small} \quad \Rightarrow \quad y \in \tilde{C} \tag{2.23}$$

and with the same argument we also have the slightly more general form of this statement

$$\Big(\forall 0<\epsilon<\rho:\ y\in\tilde{C}_{\alpha_\ell}^{(\rho-\epsilon)}\forall\alpha_\ell \text{ suff. small }\Big)\ \Rightarrow\ y\in\tilde{C}^{(\rho)}. \tag{2.24}$$

Further, from (2.21) we obtain

$$\begin{aligned}&\langle y,(A^*)^{-1}v\rangle\geq\rho\\ &\Rightarrow\ \Big(\forall 0<\epsilon<\rho:\ \langle y,R_\alpha^*v\rangle\geq\rho-\epsilon\ \forall\alpha_\ell \text{ suff. small }\Big).\end{aligned} \tag{2.25}$$

Thus we have

$$y\in\tilde{C}\ \Rightarrow\ \Big(\forall 0<\epsilon<\rho:\ y\in\tilde{C}_{\alpha_\ell}^{(\rho-\epsilon)}\forall\alpha_\ell \text{ suff. small}\Big). \tag{2.26}$$

Now, from (2.24) and (2.26) we obtain the equivalence

$$y\in\tilde{C}\ \Leftrightarrow\ \Big(\forall 0<\epsilon<\rho:\ y\in\tilde{C}_{\alpha_\ell}^{(\rho-\epsilon)}\forall\alpha_\ell \text{ suff. small}\Big). \tag{2.27}$$

Next, consider the case where $v\notin A^*(Y)$. In this case the representation of (2.16) is not defined. However, if we define

$$C_\alpha:=\{x:\ \langle R_\alpha Ax,v\rangle\geq\rho\}, \tag{2.28}$$

then since $R_\alpha Ax\to x$, $\alpha\to 0$ pointwise in X, with the same arguments as in (2.24), (2.26) and (2.27) we obtain

$$x\in C^{(\rho)}\ \Leftrightarrow\ \Big(\forall 0<\epsilon<\rho:\ x\in C_{\alpha_\ell}^{(\rho-\epsilon)}\forall\alpha_\ell \text{ suff. small}\Big). \tag{2.29}$$

From the definitions (2.17) and (2.28) we have $\tilde{C}_\alpha=AC_\alpha$, leading to

$$y\in\tilde{C}^{(\rho)}\ \Leftrightarrow\ \Big(\forall 0<\epsilon<\rho:\ y\in\tilde{C}_{\alpha_\ell}^{(\rho-\epsilon)}\forall\alpha_\ell \text{ suff. small}\Big). \tag{2.30}$$

We summarize these result as a Lemma.

LEMMA 2.4 *The regularized image class $\tilde{C}_\alpha$ tends to the image class $\tilde{C}$*

$$\tilde{C}_{\alpha_\ell}^{(\rho-\epsilon)}\to\tilde{C}^{(\rho)},\quad \ell\to\infty,\ \epsilon\to 0 \tag{2.31}$$

in the sense of (2.30).

Finally, we rewrite the representation (2.18) into

$$\begin{aligned}\tilde{C}_\alpha&=\{y\in A(X):\ \langle y,R_\alpha^*v\rangle\geq\rho\}\\ &=\Big\{y\in A(X):\ \Big\langle y,\tfrac{R_\alpha^*v}{||R_\alpha^*v||}\Big\rangle\geq\tfrac{\rho}{||R_\alpha^*v||}\Big\}.\end{aligned} \tag{2.32}$$

If $v\notin A^*Y$, then we know that

$$||R_\alpha^*v||\to\infty,\quad \alpha\to 0. \tag{2.33}$$

Due to the representation (2.32) this yields

$$\tilde{\rho}_\alpha\to 0,\quad \alpha\to 0, \tag{2.34}$$

for the distance $\tilde{\rho}_\alpha$ between $\tilde{C}_\alpha$ and zero.

THEOREM 2.5 *Consider a linear class C in X defined by its normal vector v and some distance ρ to the origin and let A be a compact linear operator $A : X \to Y$. If $v \notin A^*Y$, then the distance of $\tilde{C} = AC$ to the origin is zero.*

Proof. Since the norm of $\frac{R_\alpha^* v}{||R_\alpha^* v||}$ is bounded by one, there is a weakly convergent subsequence for $\alpha \to 0$, for which we denote the regularization parameters by α_ℓ, $\ell \in \mathbb{N}$. We call the limit element $\psi_* \in Y$. We note that for $j \in \mathbb{N}$ the element

$$y_{\alpha_j} := \psi_* \cdot 2\frac{\rho}{||\psi_*||^2 ||R_{\alpha_j}^* v||} \tag{2.35}$$

satisfies

$$\left\langle y_{\alpha_j}, \frac{R_{\alpha_\ell} v}{||R_{\alpha_\ell} v||} \right\rangle = \frac{2\rho}{||\psi_*||^2 ||R_{\alpha_j} v||} \left\langle \psi_*, \frac{R_{\alpha_\ell} v}{||R_{\alpha_\ell} v||} \right\rangle \to \frac{2\rho}{||R_{\alpha_j} v||}, \quad \ell \to \infty,$$

such that y_{α_j} is an element in $\tilde{C}_{\alpha_\ell}^{(\rho-\epsilon)}$ for all $0 < \epsilon < \rho$ and all sufficiently small $\alpha_\ell > 0$. Thus, according to (2.30), it is in $\tilde{C}^{(\rho)}$. Finally, $||y_{\alpha_j}|| \to 0$ for $j \to \infty$ proves the statement. □

Finally, we will work out the consequences of the above result for the discrimination task. Please note that we have not studied a particular algorithm yet, but worked with the general classes which are implicit in any classification algorithm.

THEOREM 2.6 *Let $U_\ell^{(1)}, U_\ell^{(2)}$ for $\ell \in \mathbb{N}$ be a sequence of halfspaces in X with distance ρ_ℓ between $U_\ell^{(1)}$ and $U_\ell^{(2)}$ for $\ell \in \mathbb{N}$. We assume that the sequence (ρ_ℓ) is bounded and that the v_ℓ which are normal to the boundary of $U_\ell^{(1)}$ and $U_\ell^{(2)}$ do not have a convergent subsequence in X. We denote the images of $U_\ell^{(1)}, U_\ell^{(2)}$ under a compact linear operator $A : X \to Y$ by $\tilde{U}_\ell^{(1)}, \tilde{U}_\ell^{(2)}$ and the distance between $\tilde{U}_\ell^{(1)}$ and $\tilde{U}_\ell^{(2)}$ by $\tilde{\rho}_\ell$ for $\ell \in \mathbb{N}$. Then, there is a subsequence ℓ_k, $k \in \mathbb{N}$ such that*

$$\tilde{\rho}_{\ell_k} \to 0, \quad k \to \infty. \tag{2.36}$$

Proof. To begin with we assume $v_\ell \in A^*(Y)$. We apply the previous theorem first to the sequence of classes $\left(U_\ell^{(1)}\right)_{\ell \in \mathbb{N}}$. We obtain a subsequence ℓ_k, $k \in \mathbb{N}$, for which the distance of its boundary to the origin tends to zero. Now, we apply the theorem again to the sequence of classifications given by $\left(U_{\ell_k}^{(2)}\right)_{k \in \mathbb{N}}$ with vectors v_{ℓ_k}. We get a subsequence ℓ_{k_j}, $j \in \mathbb{N}$, of the subsequence $(\ell_k)_{k \in \mathbb{N}}$ for which the distance of the boundary of $U_{\ell_{k_j}}^{(2)}$ to the origin tends to zero. For this subsequence, the distance between the two classes $U_{\ell_{k_j}}^{(1)}$ and $U_{\ell_{k_j}}^{(2)}$ must tend to zero for $j \to \infty$.

Secondly, consider the case where any of the v_ℓ is not in the range of A^*. In this case according to Theorem 2.5 we have $\tilde{\rho}_\ell = 0$ and (2.36) remains true. □

We have shown that in the image space Y under a compact linear operator, classification will no longer be uniformly stable even if the classes of elements are stably separable in the original space.

3. Static Magnetic Tomography

Here, we collect basic notation and results on static magnetic tomography, for more details we refer to [21], [11], [12], [13].

We represent our fuel cell or fuel cell stacks by a Lipschitz domain, Ω, in $\mathbb{R}^3$. We assume that the current j is in $L^2(\Omega)$. Its magnetic field $H(x)$ at some point $x \in \mathbb{R}^3$ is calculated by the Biot-Savart integral operator

$$(Wj)(x) = \nabla_x \times \int_\Omega \Phi(x,y) j(y)\, dy \tag{3.1}$$

where Φ is the fundamental solution

$$\Phi(x,y) = \frac{1}{4\pi|x-y|} \tag{3.2}$$

for $x \neq y \in \mathbb{R}^3$ [21]. Static magnetic tomography aims to find the current inside the domain Ω using some magnetic field measured on an open subset Λ of a surface ∂G outside of Ω, where ∂G is a smooth boundary of some domain G with $\overline{\Omega} \subset G$. The size of G depends on the measurement device but 'it is usually well separated from the cell area Ω' [11]. This leads to the *integral equation of the first kind* (c.f. [16])

$$Wj = H_{meas} \tag{3.3}$$

for j on ∂G, where H_{meas} is some magnetic field measured on ∂G. For details of how the magnetic field measurements are taken in practice, the reader is referred to [14]. As in [13] we define a region Ω_{dis} by

$$\Omega_{dis} := \left\{ y \in \mathbb{R}^3, -\frac{a_1}{2} < y_1 < \frac{a_1}{2}, -\frac{a_2}{2} < y_2 < \frac{a_2}{2}, -\frac{a_3}{2} < y_3 < \frac{a_3}{2} \right\}, \tag{3.4}$$

where $a_1, a_2, a_3 > 0$ and consider a discretization with n_i levels in the x_i direction for $i = 1, 2, 3$. We use finite integration technique (FIT) to model the currents in this discretization. This involves using Kirchoff's laws to find the current flow $\mathbf{J}$ in Ω_{dis}, see [21] for details. We employ a set $\{x_\ell \in \Lambda : \ \ell = 1, ..., M\}$ of measurement points and a grid with K wires γ_k, $k = 1, ..., K$. We find the current vector $\mathbf{J}$ with components J_k representing the current strength in each wire γ_k, $k = 1, ..., K$, using FIT. We then obtain a magnetic field vector, $\mathbf{H}$, using the definition of a discrete version of the Biot-Savart operator given by

$$(\mathbf{WJ})_\ell = -\frac{1}{4\pi} \sum_{k=1}^{K} \int_{\gamma_k} \frac{\tilde{J}_k \times (x_\ell - p)}{|x-p|^3}\, d\gamma(p), \quad \ell = 1, ..., M, \tag{3.5}$$

where $\tilde{J}_k = (J_k, 0, 0)^T$ if wire γ_k is parallel to the $x-$axis, $\tilde{J}_k = (0, J_k, 0)^T$ if wire γ_k is parallel to the $y-$axis or $\tilde{J}_k = (0, 0, J_k)^T$ if wire γ_k is parallel to the $z-$axis. The integrals can be carried out analytically [11], [13]. Thus, the linear operator $\mathbf{W} : \mathbf{J} \to \mathbf{WJ}$ mapping $\mathbb{R}^K$ into $\mathbb{R}^M$ is represented by a matrix which we also call $\mathbf{W}$. Later, we will also work with a different discretization of W by more general numerical quadrature. All proofs will work with either of these options.

Key questions on (3.3) with respect to *existence*, *uniqueness* and *stability* given H_{meas} have been investigated in a series of papers by Kühn, Kress, Potthast, Hauer,

Wannert et.al. In [12] the authors show that the nullspace contains $j := \triangle m$ for $m \in C_0^2(\Omega)$, i.e. in general our current distribution is not uniquely determined by measurements. In fact in [11] it is shown that the nullspace of the Biot-Savart operator is

$$N(W) = \{\nabla \times v : v \in H_0^1(\Omega), \nabla \cdot v = 0\}. \tag{3.6}$$

As a consequence the equation (3.3) is ill-posed in the sense of Hadamard. However in [11] it is also shown that the magnetic tomography is always uniquely solvable for discrete wire networks.

It is well-known that a compact linear operator on an infinite dimensional space cannot have a bounded inverse, compare [16]. Therefore the operator W^{-1} is unbounded and not continuous. Thus, the solution of the integral equation (3.3) does not depend stably on the measurement data and it is ill-posed.

It is common to use regularization techniques to replace W^{-1} by some bounded operator R_α with

$$\lim_{\alpha \to 0} R_\alpha W j = j, \tag{3.7}$$

where $\alpha \in \mathbb{R}$, $\alpha > 0$, is known as the *regularization parameter*. Here, we will follow [17] and employ *Tikhonov regularization* as a very popular and widely used method, where

$$R_\alpha := (\alpha I + W^* W)^{-1} W^*. \tag{3.8}$$

This defines a regularization scheme with

$$||R_\alpha|| \leq \frac{1}{2\sqrt{\alpha}}, \tag{3.9}$$

compare [6]. Tikhonov regularization projects j onto $N(W)^\perp$ [12] and so we can only reconstruct the projection onto $N(W)^\perp$ without further a priori knowledge [11]. A characterization of this space has been derived in [11] as

$$N(W)^\perp = \{j \in H_{div=0}(\Omega) : \exists q \in L^2(\Omega), \nabla \times j = \nabla q\}. \tag{3.10}$$

Different algorithms for magnetic tomography based on Tikhonov type regularization are given in [13].

It is well-known that an inherently unstable problem cannot be made stable [8]. We simply 'recover partial information about the solution as stably as possible' by use of regularization methods. We will work out next that this observation remains valid for the task of classification of fuel cells by their currents or their magnetic fields.

4. Classification for Magnetic Tomography

The goal of this section is to study classification of current densities j in some domain Ω using measurements of their magnetic fields H on a surface ∂G outside of the domain $\overline{\Omega}$. The operator which maps j to H is the Biot-Savart operator W defined in (3.1).

There are two basic options to approach the classification problem from magnetic field measurements H_{meas}, when an ill-posed problem

$$Wj = H_{meas} \tag{4.1}$$

is involved. *First*, we can use reconstruction methods to calculate an approximation j_α to the current distribution j in Ω. Then, classification methods can be applied to the reconstructed current j_α. The *second* approach is to directly apply classification in the measurement space, i.e. to the magnetic fields H_{meas}. We will work out that, as a consequence of the previous Section 2, the classifications on the magnetic fields cannot be stable, i.e. we have an *ill-posed classification problem.*

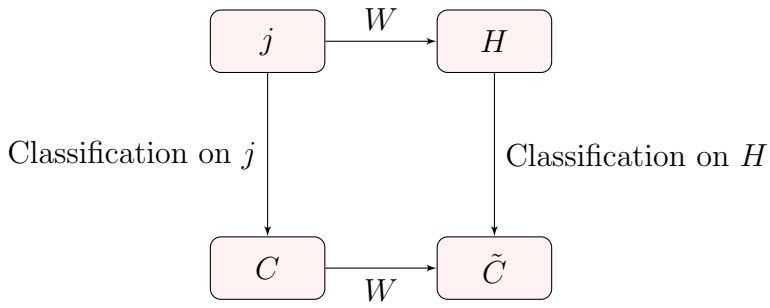

Figure 1. Classification can be carried out on the currents j directly or on the magnetic fields H. We will study the role of the ill-posedness of the equation $Wj = H$ on the behaviour of the classes C and $\tilde{C}$.

4.1. Classification via current j

Here, we describe and analyse classification of a current distribution based on sets of classes which can be grouped into levels of higher and higher precision. Assume that for the level $L \in \mathbb{N}$ we are given a set of vectors

$$\chi_1^{(L)}, ..., \chi_{n_L}^{(L)} \in L^2(\Omega), \quad n_L \in \mathbb{N} \tag{4.2}$$

with

$$\left|\left|\chi_\ell^{(L)}\right|\right| = 1, \ell = 1, ..., n_L \tag{4.3}$$

and

$$n_L \to \infty, \quad L \to \infty. \tag{4.4}$$

We study a sequence of linear classifications which are based on the vectors $\chi_\ell^{(L)}$, $\ell = 1, ..., n_L$. Given real numbers $\rho_\ell^{(L)}$, $\ell = 1, ..., n_L$, we define classes $C_\ell^{(L)}$ by

$$C_\ell^{(L)} := \left\{ j \in L^2(\Omega) : \quad \left\langle j, \chi_\ell^{(L)} \right\rangle \geq \rho_\ell^{(L)} \right\}, \quad \ell = 1, ..., n_L. \tag{4.5}$$

Further, we define a *nonlinear class* $C^{(L)}$ by

$$C^{(L)} = \bigcap_{\ell=1}^{n_L} C_\ell^{(L)}. \tag{4.6}$$

Example. As a two-dimensional example for our nonlinear class we consider the space $\mathbb{R}^2$ with two classes C_1, C_2 defined by

$$C_1 := \{\mathbf{j} \in \mathbb{R}^2 : \quad j_1 \geq \rho \text{ and } j_2 \geq \rho\} \tag{4.7}$$

and

$$C_2 := \{\mathbf{j} \in \mathbb{R}^2 : \quad j_1 < \rho \text{ or } j_2 < \rho\}, \tag{4.8}$$

where $\mathbf{j} = (j_1, j_2)^T$. This is illustrated in Figure 2.

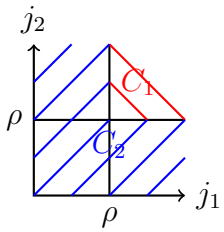

Figure 2. A linearly unseparable problem. The two classes shown cannot be separated by a line.

Clearly, this is not a linearly separable problem but it is composed of two linearly separable problems. This is illustrated in Figure 3, where we see that $C_1 = C \cap C'$ and C_2 simply consists of all input vectors that do not lie in C_1.

Figure 3. The unseparable problem shown in Figure 2 can be broken down into 2 linearly separable problems.

In particular, let us consider a hierarchy of subsets $\Omega_\ell^{(L)}$, $\ell = 1, ..., n_L$ for $L \in \mathbb{N}$ of Ω such that the sets are disjoint on each level, i.e.

$$\Omega_\ell^{(L)} \cap \Omega_m^{(L)} = \emptyset \text{ for } \ell \neq m, \tag{4.9}$$

we have a real refinement moving from level L to $L+1$, i.e.

$$\forall \ell = 1, ..., n_L \; \exists \; m \in \{1, ..., n_{L+1}\} \text{ such that } \Omega_\ell^{(L+1)} \subset \Omega_m^{(L)} \tag{4.10}$$

and the subsets on each level add up to the full set Ω, i.e.

$$\Omega = \bigcup_{\ell=1}^{n_L} \Omega_\ell^{(L)} \tag{4.11}$$

for every $L \in \mathbb{N}$. With the area or volume $\left|\Omega_\ell^{(L)}\right|$, respectively, of some set $\Omega_\ell^{(L)}$ we define

$$\chi_\ell^{(L)}(x) := \begin{cases} \frac{1}{\left|\Omega_\ell^{(L)}\right|^{1/2}}, & x \in \Omega_\ell^{(L)}, \\ 0, & \text{otherwise.} \end{cases} \tag{4.12}$$

the functions $\chi_\ell^{(L)}$ are in $L^2(\Omega)$ for $\ell = 1, ..., n_L$ and $L \in \mathbb{N}$. Then we have

$$\left|\left|\chi_\ell^{(L)}\right|\right|_{L^2(\Omega)} = 1 \tag{4.13}$$

We now collect all vectors $\chi_\ell^{(L)}$ for $\ell = 1, ..., n_L$ and $L = 1, 2, 3, ...$ into one sequence, for which we use the letter v_k, $k \in \mathbb{N}$.

For the fuel cell application nonlinear classes will naturally appear when the flow through the cell membrane is monitored. For example, the vectors $\chi_\ell^{(L)}$ can be chosen to be the special basis used for current reconstructions by Wannert and Potthast [22]. Here, the class $C_\ell^{(L)}$ is the set of all currents which have a component larger than $\rho_\ell^{(L)}$ along the direction $\chi_\ell^{(L)} \in L^2(\Omega)$. Good cells are those where we have a homogeneous distribution of the current, which means that all components are larger than some threshold ρ. This corresponds to the nonlinear class C defined in (4.6), which is composed of a sequence of linear classes.

We may choose a hierarchy of finer and finer discretizations to test the homogeneity by using the sequence v_k, $k \in \mathbb{N}$ defined in (4.12). Clearly, the discretization in the space of current densities is perfectly stable and when we distinguish currents which have components larger than ρ from those smaller than $\rho - \epsilon$, we obtain stably separable classes in the space X of current densities. In the next section we will see that this is no longer the case when we try to classify these classes by their magnetic field values.

As a preparation to the next section, where we want to use Theorem 2.6, we state the following result.

LEMMA 4.1 *The sequence v_k defined via (4.12) does not contain a convergent subsequence in $L^2(\Omega)$.*

Proof. Assume there exists a convergent subsequence v_{k_i} of $(v_k)_{k\in\mathbb{N}}$, i.e. there is some element $v_* \in L^2(\Omega)$ such that

$$||v_* - v_{k_i}||_{L^2(\Omega)} \to 0, \quad i \to \infty. \tag{4.14}$$

We remark that the volume (or area, respectively) of the support $\text{supp}(v_{k_i})$ tends to zero for $i \to \infty$. Then the support of v_* must be zero as well, but for L^2 functions that cannot be the case. Thus, a convergent subsequence does not exist. □

4.2. Classification via magnetic field H

For applications, a basic task is to classify current distributions from their magnetic field $H \in L^2(\partial G)$. Here, we would like to work with the classes

$$\begin{aligned} C_k^{(1)} &:= \{y \in A(X) : \ \langle A^{-1}y, v_k\rangle \geq \rho\}, \\ C_k^{(2)} &:= \{y \in A(X) : \ \langle A^{-1}y, v_k\rangle \leq \rho - \epsilon\}, \end{aligned} \tag{4.15}$$

for $k \in \mathbb{N}$ defined by the vectors (4.12). However, the corresponding image classes $\tilde{C}_k^{(j)} = AC_k^{(j)}$, $j = 1, 2$, are no longer stably separable.

THEOREM 4.2 *Consider a classification algorithm based on the current vectors v_k defined via (4.12). Then, the distance $\tilde{\rho}_k$ of the image classes $\tilde{C}_k^{(1)}$ and $\tilde{C}_k^{(2)}$ in $L^2(\partial G)$ is $\tilde{\rho}_k = 0$.*

Proof. We show that v_k cannot be in the image of the adjoint W^* of the Biot-Savart integral operator. We rewrite W as

$$(Wj)(x) = \sum_{\xi,p,\eta} e_\xi \epsilon_{\xi p\eta} \int_\Omega \partial_{x_p} \left(\Phi(x,y)\right) j_\eta(y) dy, \tag{4.16}$$

where the sum is over $\xi, p, \eta = 1, ..., 3$ and $\epsilon_{\xi p\eta}$ is the total antisymmetric tensor, i.e. it is 1 if ξ, p, η is an even permutation of $1, 2, 3$, it is -1 if the permutation is odd and it is zero if any two of the indices are the same. Thus, the adjoint of W is given by

$$(W^*\psi)(y) = \sum_{\xi,p,\eta} \int_{\partial G} \psi_\xi(x) \epsilon_{\xi p\eta} \partial_{x_p} \Phi(x,y) e_\eta \, ds(x), \quad y \in \Omega. \tag{4.17}$$

The operator has an analytic kernel. Since the function v_k is discontinuous at the boundary $\partial\Omega_\ell^{(L)}$ of its support $\Omega_\ell^{(L)}$ with appropriately chosen parameters L and ℓ, the vector v_k cannot be in the image of W^*. Now, by an application of Theorem 2.5 we obtain that both classes have distance zero to the origin, which yields $\tilde{\rho}_k = 0$ and ends the proof. □

Finally, we remark that classification by magnetic fields will also be unstable if vectors $v_k \in W^*(L^2(\partial G))$ are chosen. In this case classification for one single direction v_k for k fixed will be stable, but if we choose a sequence of directions v_k, $k = 1, ..., n$ without convergent subsequence, then for $n \to \infty$ the distance $\tilde{\rho}_k$ between two image classes $C_k^{(1)}$ and $C_k^{(2)}$ of the classification must satisfy

$$\tilde{\rho}_k \to 0, \quad k \to \infty, \tag{4.18}$$

in the same way as in Theorem 2.6.

The above phenomenon corresponds to well-known effects in the numerical treatment of ill-posed problems. When projection methods are used, a refinement of the discretization which us achieved by using a larger projection space increases the ill-conditioning of the corresponding matrices. This increase is exponential for exponentially ill-posed problems, as we have in the case of magnetic tomography. Here, a refinement in the classification leads to stronger instability and reduced separability.

5. On the Ill-Posedness of Fisher's Linear Discriminant for Remote Data

So far we have studied the ill-posedness of classification problems which can be based on linear classification. We have shown that in general linear compact operators map stably separable problems into classifications which are no longer stably separable. However, we have not yet studied a particular algorithm for such classifications.

The task of this section is to investigate a well-known scheme for supervised classification 2.1 known as *Fisher's Linear Discriminant*. We will show that the method is also ill-posed in the sense that for an increased number of measurement points the norm of the inverse operators employed by the method become unbounded. As a particular application, we will apply the method to the problem of fuel cell classification and investigate the relationship between different ways to regularize the problem.

5.1. Fisher's Linear Discrimination on j and H

Fisher's linear discriminant is not strictly speaking a discriminant but rather a method of *reducing the dimensionality* of the input space in such a way that we have maximum class separation in the new space. We call this the *reduction step* or *step one*. Once we have performed this dimensionality reduction we can use the projected data to *construct a discriminant*, compare [2]. This is denoted as the *discrimination step* or *step two*. Dimensionality reduction is desirable for example of the application of classification algorithms to the problem of quality control of *fuel cells*, since we will typically be working in a high dimensional input space.

We consider the two class case, so for example class C_1 represents 'working' and class C_2 represents 'not working'. Suppose the training set contains the training vectors $\boldsymbol{\beta}_\xi^{(\omega)}$ for $\omega = 1, \ldots, N_\xi$ for the two classes C_ξ with $\xi = 1, 2$. In the *reduction step* we project $\boldsymbol{\beta}_\xi^{(\omega)}$ into a one dimensional space by

$$y_\xi^{(\omega)} = \mathbf{w}^T \boldsymbol{\beta}_\xi^{(\omega)}, \tag{5.1}$$

where $\mathbf{w}$ is some *weight vector* to be determined. For linearly separable classes such a vector $\mathbf{w}$ will always exist, it is the normal vector to the hyperplane separating the two classes.

The basic target of Fisher's linear discriminant is to avoid losing too much information when projecting the input vectors. To achieve this we aim to choose $\mathbf{w}$ such that we have maximum class separation [2] by considering parameters in both the input space and the projection space. This is carried out as follows.

DEFINITION 5.1 *Assume that we have N_ξ input vectors $\boldsymbol{\beta}_\xi^{(\omega)}$, $\omega = 1, ..., N_\xi$, in each class C_ξ for $\xi = 1, 2$, then the mean of this training set before projection is*

$$\mathbf{m}_\xi = \frac{1}{N_\xi} \sum_{\omega=1}^{N_\xi} \boldsymbol{\beta}_\xi^{(\omega)}, \tag{5.2}$$

where N_ξ is the number of training vectors for class C_ξ. Given $\mathbf{w}$, the projected class mean is then

$$m_\xi = \mathbf{w}^T \mathbf{m}_\xi. \tag{5.3}$$

Furthermore, we define matrices $\mathbf{S}_\xi$ and scalars s_ξ which measure the scatter of class C_ξ before and after projection respectively

$$\mathbf{S}_\xi = \frac{1}{N_\xi - 1} \sum_{\omega=1}^{N_\xi} (\boldsymbol{\beta}_\xi^{(\omega)} - \mathbf{m}_\xi)(\boldsymbol{\beta}_\xi^{(\omega)} - \mathbf{m}_\xi)^T \tag{5.4}$$

$$s_\xi^2 = \frac{1}{N_\xi - 1} \sum_{\omega=1}^{N_\xi} (y_\xi^{(\omega)} - m_\xi)^2, \tag{5.5}$$

where y_ξ is given by (5.1).

Note that in contrast to parts of the literature about Fischer's Linear Discriminant here we have used the scaling by $1/(N_\xi - 1)$, $\xi = 1, 2$. With this scaling the quantity $\mathbf{S}_\xi$ is an estimator for the covariance matrix and we as long as $N_1 = N_2$ the constant does not change the arguments leading to Fischer's linear discriminant.

Fischer's Linear Discriminant simultaneously maximizes the distance between the mean values of the two clusters and minimizes the variance of the input vectors in each class around their respective mean values. This is used as a heuristical approach to determining $\mathbf{w}$. The so-called *Fisher's criterion* is the functional

$$\begin{aligned} \mu(\mathbf{w}) &= \frac{(m_2 - m_1)^2}{s_1^2 + s_2^2} \\ &= \frac{\mathbf{w}^T \mathbf{S}_B \mathbf{w}}{\mathbf{w}^T \mathbf{S}_F \mathbf{w}}, \end{aligned} \tag{5.6}$$

where $\mathbf{S}_F = \mathbf{S}_1 + \mathbf{S}_2$ is the *within-class scatter matrix* and $\mathbf{S}_B = (\mathbf{m}_2 - \mathbf{m}_1)(\mathbf{m}_2 - \mathbf{m}_1)^T$ is the *between-class scatter matrix*. Maximizing Fisher's criterion with respect to $\mathbf{w}$ (c.f. [2], [9]) leads to

$$\mathbf{w} \propto \mathbf{S}_F^{-1}(\mathbf{m}_2 - \mathbf{m}_1). \tag{5.7}$$

Given a training set, we calculate $\mathbf{m}_\xi$, $\xi = 1, 2$ according to (5.2) and $\mathbf{w}$ according to (5.7). Then, we employ (5.1) to complete the *reduction step*, which yields a one-dimensional version of our training set. In the *second step* we calculate a discrimination boundary based on the values $y_\xi^{(w)}$. There are several methods to do this last step, compare [2]. The *second step* is carried out on a one-dimensional space, and it is well-posed in general.

The *reduction step*, however, is usually ill-posed, when applied to data in some image space under a compact linear operator as for magnetic tomography. In this case the training set $\boldsymbol{\beta}_\xi^{(\omega)}$ consists of a discretized version $\mathbf{H}$ of magnetic fields $H = Wj$. We obtain the vector $\mathbf{H}$ by choosing mesurement points $x_k \in \Lambda$ and then sorting the Cartesian components of $H(x_k)$ in the form

$$\mathbf{H} = \Big(H_1(x_1), H_2(x_1), H_3(x_1), H_1(x_2), ...\Big)^T. \tag{5.8}$$

We will complete this section by a rigorous proof showing that in this case the norm of the inverse $\mathbf{S}_F^{-1}$ of $\mathbf{S}_F = \mathbf{S}_F^{(\mathbf{H},M)}$ tends to infinity when the number of discretization points M, i.e. the dimension of the space of training vectors $\boldsymbol{\beta}_\xi^{(\omega)}$, tends to infinity.

THEOREM 5.2 *Consider the dependence of the matrix* $\mathbf{S}_F^{(\mathbf{H})} = \mathbf{S}_F^{(\mathbf{H},M)}$ *on the dimension of the space of training vectors* $\mathbb{R}^{3M}$*, where* M *is the number of measurement points on* Λ*. Then we have*

$$\left|\left|\left(\mathbf{S}_F^{(\mathbf{H},M)}\right)^{-1}\right|\right|_\infty \to \infty, \quad M \to \infty. \tag{5.9}$$

Proof. The key tool for showing the result (5.9) is given in Lemma 5.6 below, showing that if we have the inverse A_M^{-1} of a sequence of operators A_M which is converging pointwise towards some compact linear operator A, then

$$\left|\left|A_M^{-1}\right|\right| \to \infty, \quad M \to \infty. \tag{5.10}$$

To construct a continuous operator for the covariance matrix $\mathbf{S}_F^{(\mathbf{H},M)}$ we remark that within our framework a training vector $\mathbf{H}_\xi^{(\omega)}$ with $\xi \in \{1,2\}$ and $\omega \in \{1,...,N_\xi\}$ is arizing from a true current $j_\xi^{(\omega)} \in (C(\Omega))^3$ (for real data as training set) or some numerical approximation of it (for simulated data for training). For the two classes C_ξ, $\xi = 1,2$, we define the integral operators

$$\begin{aligned}(S_\xi^{(j)}\varphi)(z,k) := \frac{1}{N_\xi - 1}\sum_{\omega=1}^{N_\xi}\sum_{\ell=1}^{3}\int_\Omega \left(j_{\xi,k}^{(\omega)}(z) - \overline{j}_{\xi,k}(z)\right) \\ \cdot \left(j_{\xi,\ell}^{(\omega)}(y) - \overline{j}_{\xi,\ell}(y)\right)\varphi_\ell(y)\, dy\end{aligned} \tag{5.11}$$

and

$$\begin{aligned}(S_\xi^{(H)}\psi)(x,k) := \frac{1}{N_\xi - 1}\sum_{\omega=1}^{N_\xi}\sum_{\ell=1}^{3}\int_\Lambda \left(H_{\xi,k}^{(\omega)}(x) - \overline{H}_{\xi,k}(x)\right) \\ \cdot \left(H_{\xi,\ell}^{(\omega)}(y) - \overline{H}_{\xi,\ell}(y)\right)\psi_\ell(y)\, ds(y)\end{aligned} \tag{5.12}$$

for $z \in \Omega$, $x \in \Lambda$ and $k \in \{1,2,3\}$. Then, we set

$$\begin{aligned}S_F^{(j)} &:= S_1^{(j)} + S_2^{(j)} \\ S_F^{(H)} &:= S_1^{(H)} + S_2^{(H)}.\end{aligned} \tag{5.13}$$

Using $H = Wj$ we readily verify

$$S_F^{(H)} = W S_F^{(j)} W^*. \tag{5.14}$$

LEMMA 5.3 *Assume that* Ω *is a bounded set and all* $j_\xi^{(\omega)}$, $\omega = 1,...,N$, $\xi = 1,2$ *are uniformly bounded on* Ω *by some constant* C*, then the operator* $S_F^{(j)}$ *is a bounded operator in* $(C(\Omega))^3$*.*

Proof. We estimate

$$\sup_{z\in\Omega,k=1,2,3}\left|S_F^{(j)}\varphi(z,k)\right| \le C^2 \cdot \left(\int_\Omega 1\, dy\right) \cdot ||\varphi||_\infty,$$

from which the statement follows. □

Since $W : (C(\Omega))^3 \to (C(\Lambda))^3$ is compact and $W^* : (C(\Lambda))^3 \to (C(\Omega))^3$ is compact as well, the operator $S_F^{(H)}$ is compact in $(C(\Lambda))^3$.

A discretization of this operator is achieved by using numerical quadrature for all three of its factors. With nodes z_κ, $\kappa = 1, ..., M$ in Ω and quadrature weights s_κ we discretize x via z_ι and y via z_κ. Then, the operator $S_F^{(j)}$ is approximated via the matrix

$$\mathbf{S}_F^{(\mathbf{j},M)} := \left(\sum_{\xi=1,2} \frac{1}{N_\xi - 1} \left(\sum_{\omega=1}^{N_\xi} \left(j_\xi^{(\omega)}(z_\iota) - \overline{j}_\xi(z_\iota) \right) \left(j_\xi^{(\omega)}(z_\kappa) - \overline{j}_\xi(z_\kappa) \right)^T s_\kappa \right) \right)_{\iota,\kappa=1,...,M.}$$

Note that $\mathbf{S}_F^{(\mathbf{j},M)}$ is an $M \times M$-matrix of 3×3 matrices, i.e. it is a $3M \times 3M$-matrix operating on $\mathbb{R}^{3M}$. If the quadrature formula is convergent for $x = z_\iota$ we obtain

$$(\mathbf{S}_F^{(\mathbf{j},M)} \boldsymbol{\varphi})_\iota \to S_F^{(j)} \varphi(x), \quad M \to \infty, \tag{5.15}$$

where we employ the *projection operator*

$$P_\Omega^{(M)} : (C(\Omega))^3 \to \mathbb{R}^{3M}, \quad \varphi \mapsto \boldsymbol{\varphi} = (\boldsymbol{\varphi}_\kappa)_{\kappa=1,...,M} \tag{5.16}$$

with $\boldsymbol{\varphi}_\kappa := \varphi(z_\kappa) \in \mathbb{R}^3$ for $\kappa = 1, ..., M$. Further, assume that $Q_\Omega^{(M)}$ is a bounded *interpolation operator* $\mathbb{R}^M \to C(\Omega)$ for scalar functions or $\mathbb{R}^{3M} \to (C(\Omega))^3$ in the vectorial case, based on the nodes $z_\kappa \in \Omega$, $\kappa = 1, ..., M$, where we have

$$||Q_\Omega^{(M)} \boldsymbol{\varphi}||_\infty \le c ||\boldsymbol{\varphi}||_\infty \tag{5.17}$$

with some constant c uniformly for $M \in \mathbb{N}$. Further, we assume that we have convergence of the interpolation operator in the sense that

$$||Q_\Omega^{(M)} P_\Omega^{(M)} \varphi - \varphi||_\infty \to 0, \quad M \to \infty. \tag{5.18}$$

On a regular grid in two or three dimensions such an operator with $c = 1$ is obtained by piecewise linear interpolation along the canonical axes. We now combine the interpolation operator with $\mathbf{S}_F^{(\mathbf{j},M)}$ to obtain the following pointwise convergence result.

LEMMA 5.4 *The operator $Q_\Omega^{(M)} \mathbf{S}_F^{(\mathbf{j},M)} P^{(M)}$ is pointwise convergent towards $S_F^{(j)}$ in $(C(\Omega))^3$, i.e. we have*

$$Q_\Omega^{(M)} \mathbf{S}_F^{(\mathbf{j},M)} P_\Omega^{(M)} \varphi \to S_F^{(j)} \varphi, \quad M \to \infty, \quad \text{in } C(\Omega). \tag{5.19}$$

Proof. The statement is a result of (5.15) and the convergence of the interpolation operator (5.18) applied to the continuous function $S_F^{(j)} \varphi$. □

To construct an interpolation operator when Λ is a smooth two-dimensional surface surrounding Ω, we can use local parametrizations and a triangularization in the space $\mathbb{R}^2$ which takes the nodes x_η, $\eta = 1, ..., M$ as nodes of the triangles. On a triangle we employ a linear interpolation, which is then mapped back into $\mathbb{R}^3$ with a norm bounded

uniformly for all $\tilde{M} \in \mathbb{N}$, such that (5.20) is satisfied. We denote an interpolation operator on Λ by $Q_\Lambda^{(\tilde{M})}$ and assume to have

$$||Q_\Lambda^{(\tilde{M})}\boldsymbol{\psi}||_\infty \leq c||\boldsymbol{\psi}||_\infty \tag{5.20}$$

with some constant c uniformly for $\tilde{M} \in \mathbb{N}$ and a result analogous to (5.18).

The continuous form of the Biot-Savart operator W is given by (3.1). A discretization of W via standard quadrature or via finite integration technique leads to some matrix $\mathbf{W}$ for W and to a matrix $\mathbf{W}^*$ for W^*. In the same way as in Lemma 5.4 we obtain the following result.

LEMMA 5.5 *The operator $Q_\Lambda^{(M)}\mathbf{W}^{(M)}P_\Omega^{(M)}$ is pointwise convergent towards W as operator $(C(\Omega))^3 \to (C(\Lambda))^3$, i.e. for fixed $\varphi \in (C(\Omega))^3$ we have*

$$Q_\Lambda^{(M)}\mathbf{W}^{(M)}P_\Omega^{(M)}\varphi \to W\varphi, \quad M \to \infty, \quad \text{in } (C(\Lambda))^3. \tag{5.21}$$

The operator $Q_\Omega^{(M)}\mathbf{W}^{*(M)}P_\Lambda^{(M)}$ is pointwise convergent towards W^* as operator $(C(\Lambda))^3 \to (C(\Omega))^3$, i.e. for fixed $\psi \in (C(\Lambda))^3$ we have

$$Q_\Omega^{(M)}\mathbf{W}^{*(M)}P_\Lambda^{(M)}\psi \to W^*\psi, \quad M \to \infty, \quad \text{in } (C(\Omega))^3. \tag{5.22}$$

We now consider the discretized version of the product $WS_F^{(j)}W^*$ as a mapping $(C(\Lambda))^3 \to (C(\Lambda))^3$. We remark that we have $P_\Omega^{(M)}Q_\Omega^{(M)} = I^{(3M)}$ where $I^{(3M)}$ denotes the identity in $\mathbb{R}^{3M}$. This yields

$$\begin{aligned} &Q_\Lambda^{(M)}\mathbf{W}^{(M)}\mathbf{S}_F^{(\mathbf{j},M)}\mathbf{W}^{*(M)}P_\Lambda^{(M)} \\ &= \left(Q_\Lambda^{(M)}\mathbf{W}^{(M)}P_\Omega^{(M)}\right)\left(Q_\Omega^{(M)}\mathbf{S}_F^{(\mathbf{j},M)}P_\Omega^{(M)}\right)\left(Q_\Omega^{(M)}\mathbf{W}^{*(M)}P_\Lambda^{(M)}\right). \end{aligned} \tag{5.23}$$

Since we have pointwise convergence of all three operators, we obtain pointwise convergence of the product. We are now able to study the ill-posedness of the discretized operator using the general result of Lemma 5.6.

We now complete the proof of Theorem 5.2. We first note that according to Lemma 5.6 the inverse of the operator $Q_\Lambda^{(M)}\mathbf{W}^{(M)}\mathbf{S}_F^{(\mathbf{j},M)}\mathbf{W}^{*(M)}P_\Lambda^{(M)}$ cannot be uniformly bounded for $M \to \infty$. Finally, since $Q_\Lambda^{(M)}$ and $P_\Lambda^{(M)}$ are uniformly bounded for $M \in \mathbb{N}$, and by

$$Q_\Lambda^{(M)}\left(\mathbf{W}^{(M)}\mathbf{S}_F^{(\mathbf{j},M)}\mathbf{W}^{*(M)}\right)^{-1}P_\Lambda^{(M)} = \left(Q_\Lambda^{(M)}\mathbf{W}^{(M)}\mathbf{S}_F^{(\mathbf{j},M)}\mathbf{W}^{*(M)}P_\Lambda^{(M)}\right)^{-1}, \tag{5.24}$$

the discrete matrix $\left(\mathbf{W}^{(M)}\mathbf{S}_F^{(\mathbf{j},M)}\mathbf{W}^{*(M)}\right)^{-1}$ cannot be boundedly invertible either, which completes the proof. □

Above we needed the following result to investigate the ill-posedness of Fisher's linear discriminant when applied to magnetic fields.

LEMMA 5.6 *Let $W : X \to X$ be a compact linear operator where X is a Banach space. Let $W_N : X \to X$ be a family of operators which are invertible on a subspace $X_N \subset X$ of dimension N, such that W_N tends to W pointwise. Then*

$$\left|\left|W_N^{-1}\right|\right| \to \infty \tag{5.25}$$

as $N \to \infty$.

Proof. Assume $\left|\left|W_N^{-1}\right|\right| \leq C$ for all $N \in \mathbb{N}$. Since W is compact, there exists some sequence $(\varphi_n) \subset X$ with $||\varphi_n|| = 1$ such that

$$W\varphi_n \to 0 \tag{5.26}$$

as $n \to \infty$. Furthermore, since $W_N \to W$ pointwise, for every fixed $n \in \mathbb{N}$ we have

$$W_N\varphi_n \to W\varphi_n \tag{5.27}$$

as $N \to \infty$. Therefore $\forall \epsilon > 0$, $\exists n_\epsilon$ such that $\forall n \geq n_\epsilon$

$$||W\varphi_n|| \leq \frac{\epsilon}{2} \tag{5.28}$$

and choosing one fixed $n \geq n_\epsilon$ there is N_ϵ such that $\forall N \geq N_\epsilon$

$$||W_N\varphi_n - W\varphi_n|| \leq \frac{\epsilon}{2}. \tag{5.29}$$

Thus $\forall \epsilon > 0$ $\exists n$ and N_ϵ such that $\forall N \geq N_\epsilon$

$$||W\varphi_n|| + ||W_N\varphi_n - W\varphi_n|| \leq \epsilon. \tag{5.30}$$

Thus

$$||W_N\varphi_n|| \leq ||W\varphi_n|| + ||W_N\varphi_n - W\varphi_n|| \leq \epsilon. \tag{5.31}$$

Choosing $\psi_n = W_N\varphi_n$ we obtain

$$\begin{aligned}\left|\left|W_N^{-1}\right|\right| &= \sup_{||\psi_n||\neq 0} \frac{\left|\left|W_N^{-1}\psi_n\right|\right|}{||\psi_n||} = \sup_{||\psi_n||\neq 0} \frac{\left|\left|W_N^{-1}\psi_n\right|\right|}{\left|\left|W_N^{-1}W_N\psi_n\right|\right|} \\ &\geq \frac{\left|\left|W_N^{-1}\psi_n\right|\right|}{\left|\left|W_NW_N^{-1}\psi_n\right|\right|} = \frac{||\varphi_n||}{||W_N\varphi_n||} = \frac{1}{||W_N\varphi_n||}.\end{aligned} \tag{5.32}$$

Thus

$$\left|\left|W_N^{-1}\right|\right| \geq \frac{1}{\epsilon} \tag{5.33}$$

and so $\left|\left|W_N^{-1}\right|\right|$ cannot be bounded. □

5.2. Comparison of the two approaches

The goal of this part is to work out the analysis to compare the two approaches to the classification problem, i.e.

(i) *Classification after the reconstruction*: first reconstruct the current densities j and then carry out a classification on the reconstructed current densities,

(ii) *Classification on the field data*: Apply the classification directly to the magnetic field data.

We will first look at the unregularized problem and then study their relation when Tikhonov regularization is applied. We will find that the unregularized approaches are equivalent, but of course they are not practically applicable since the ill-posedness needs to be taken care of. We prove that the regularized versions cannot be equivalent.

THEOREM 5.7 *The unregularized Fisher's linear discriminant algorithm applied to the magnetic field vectors is equivalent to the algorithm applied to the currents which are reconstructed from the magnetic fields by an unregularized inversion of the operator B.*

Proof. For the classification task we start with the samples $\mathbf{H}^{(\omega)}$. When we carry out the reconstruction by a numerical method, the corresponding currents are linked to these by

$$\mathbf{H}^{(\omega)} = \mathbf{B}\boldsymbol{\beta}^{(\omega)} = \mathbf{W}\mathbf{J}\left(\boldsymbol{\beta}^{(\omega)}\right), \tag{5.34}$$

where $\mathbf{W}$ is a discretized version of the Biot-Savart operator and $\mathbf{J}$ and $\mathbf{B}$ are discretized current and magnetic field matrices respectively. Then, the scatter matrix for the approach in the image space is

$$\begin{aligned}\mathbf{S}_F^{(\mathbf{H})} &= \sum_{\xi=1,2}\sum_{\mathbf{H}^{(\omega)}\in C_\xi}\left(\mathbf{H}^{(\omega)} - \mathbf{m}_\xi^{(\mathbf{H})}\right)\left(\mathbf{H}^{(\omega)} - \mathbf{m}_\xi^{(\mathbf{H})}\right)^T \\ &= \sum_{\xi=1,2}\sum_{\boldsymbol{\beta}^{(\omega)}\in C_\xi}\left(\mathbf{W}\mathbf{J}\boldsymbol{\beta}^{(\omega)} - \mathbf{W}\mathbf{J}\mathbf{m}_\xi^{(\boldsymbol{\beta})}\right)\left(\mathbf{W}\mathbf{J}\boldsymbol{\beta}^{(\omega)} - \mathbf{W}\mathbf{J}\mathbf{m}_\xi^{(\boldsymbol{\beta})}\right)^T \end{aligned} \tag{5.35}$$

where $\mathbf{m}_\xi^{(\mathbf{H})}$ and $\mathbf{m}_\xi^{(\boldsymbol{\beta})}$ represent the means of the magnetic field and basis function coefficient classes respectively. Therefore

$$\begin{aligned}\mathbf{S}_F^{(\mathbf{H})} &= \mathbf{W}\mathbf{J}\mathbf{S}_F^{(\boldsymbol{\beta})}\mathbf{J}^T\mathbf{W}^T \\ &= \mathbf{B}\mathbf{S}_F^{(\boldsymbol{\beta})}\mathbf{B}^T. \end{aligned} \tag{5.36}$$

If we substitute (5.36) into (5.7) we find that the classification vector $\mathbf{w}^{(\mathbf{H})}$ in the image space is given by

$$\begin{aligned}\mathbf{w}^{(\mathbf{H})} &\propto \left(\mathbf{S}_F^{(\mathbf{H})}\right)^{-1}\left(\mathbf{m}_2^{(\mathbf{H})} - \mathbf{m}_1^{(\mathbf{H})}\right) \\ &= \left(\mathbf{B}\mathbf{S}_F^{(\boldsymbol{\beta})}\mathbf{B}^T\right)^{-1}\left(\mathbf{m}_2^{(\mathbf{H})} - \mathbf{m}_1^{(\mathbf{H})}\right), \end{aligned} \tag{5.37}$$

where $\mathbf{w}^{(\mathbf{H})}$ represents the weight vector found by applying Fisher's linear discriminant to $\mathbf{H}$. Then

$$\begin{aligned}\mathbf{w}^{(\mathbf{H})} &\propto \left(\mathbf{B}^T\right)^{-1}\left(\mathbf{S}_F^{(\boldsymbol{\beta})}\right)^{-1}\mathbf{B}^{-1}\left(\mathbf{W}\mathbf{J}\mathbf{m}_2^{(\boldsymbol{\beta})}-\mathbf{W}\mathbf{J}\mathbf{m}_1^{(\boldsymbol{\beta})}\right)\\ &= \left(\mathbf{B}^T\right)^{-1}\left(\mathbf{S}_F^{(\boldsymbol{\beta})}\right)^{-1}\left(\mathbf{m}_2^{(\boldsymbol{\beta})}-\mathbf{m}_1^{(\boldsymbol{\beta})}\right).\end{aligned} \tag{5.38}$$

It is linked to the classification vector $\mathbf{w}^{(\beta)}$ in the input space by

$$\mathbf{w}^{(\mathbf{H})} \propto \left(\mathbf{B}^T\right)^{-1}\mathbf{w}^{(\boldsymbol{\beta})}, \tag{5.39}$$

which is a discrete version of (2.9). Classification in the image space given some data $\mathbf{H}$ is carried out by calculating $(\mathbf{w}^{(\mathbf{H})})^T\mathbf{H}$. In the state space it is given by

$$\left(\mathbf{w}^{(\boldsymbol{\beta})}\right)^T\boldsymbol{\beta} = \left(\mathbf{w}^{(\boldsymbol{\beta})}\right)^T\mathbf{B}^{-1}\mathbf{H} = \left(\mathbf{w}^{(\mathbf{H})}\right)^T\mathbf{H}, \tag{5.40}$$

which proves the theorem. □

Finally, we need to study the relation between the two regularized versions of Fisher's linear discriminant. The first version uses Tikhonov regularization directly applied to invert $\mathbf{S}_F^{(\mathbf{H})}$, i.e. we calculate

$$R_\alpha^{(\mathbf{H})} := \left(\alpha I + \left(\mathbf{S}_F^{(\mathbf{H})}\right)^*\mathbf{S}_F^{(\mathbf{H})}\right)^{-1}\left(\mathbf{S}_F^{(\mathbf{H})}\right)^*, \quad \alpha > 0. \tag{5.41}$$

The regularized version of (5.37) is thus given by

$$\mathbf{w}_\alpha^{(\mathbf{H})} := R_\alpha^{(\mathbf{H})}\left(\mathbf{m}_2^{(\mathbf{H})}-\mathbf{m}_1^{(\mathbf{H})}\right). \tag{5.42}$$

The second version applies the discrimination algorithm to the reconstructed coefficients, i.e. it uses

$$\boldsymbol{\beta}_\alpha^{(\omega)} := \left(\alpha\mathbf{I}+\mathbf{B}^T\mathbf{B}\right)^{-1}\mathbf{B}^T\mathbf{H}^{(\omega)}, \quad \alpha > 0. \tag{5.43}$$

We define $\mathbf{m}_{\xi,\alpha}$ as the mean of the $\boldsymbol{\beta}_\alpha^{(\omega)}$ for C_ξ and

$$\mathbf{S}_{\xi,\alpha}^{(\boldsymbol{\beta})} := \sum_{\boldsymbol{\beta}^{(\omega)}\in C_\xi}\left(\boldsymbol{\beta}_\alpha^{(\omega)}-\mathbf{m}_{\xi,\alpha}\right)\left(\boldsymbol{\beta}_\alpha^{(\omega)}-\mathbf{m}_{\xi,\alpha}\right)^T \tag{5.44}$$

for $\xi = 1, 2$ and $\mathbf{S}_{F,\alpha}^{(\boldsymbol{\beta})} = \mathbf{S}_{1,\alpha}^{(\boldsymbol{\beta})} + \mathbf{S}_{2,\alpha}^{(\boldsymbol{\beta})}$ as usual. Then, we calculate

$$\mathbf{S}_{F,\alpha}^{(\boldsymbol{\beta})} = \left(\alpha\mathbf{I}+\mathbf{B}^T\mathbf{B}\right)^{-1}\mathbf{B}^T\mathbf{S}_F^{(\mathbf{H})}\mathbf{B}\left(\alpha\mathbf{I}+\mathbf{B}^T\mathbf{B}\right)^{-1}. \tag{5.45}$$

Now, the second version calculates a regularized verson of the discrimination vector $\mathbf{w}^{(\boldsymbol{\beta})}$ by

$$\mathbf{w}_\alpha^{(\boldsymbol{\beta})} := \left(\mathbf{S}_{F,\alpha}^{(\boldsymbol{\beta})}\right)^{-1}\left(\mathbf{m}_{2,\alpha}^{(\boldsymbol{\beta})}-\mathbf{m}_{1,\alpha}^{(\boldsymbol{\beta})}\right). \tag{5.46}$$

LEMMA 5.8 *The two regularizations of the discrimination problem for magnetic tomography are not equivalent, in the sense that in general they will not provide identical classifications, even if all corresponding parameters and discretizations are chosen appropriately.*

Proof. The classifications can only be equivalent, if the classification vectors satisfy (5.39). To show that this in general cannot be the case when regularized calculations are carried out, we study the behaviour of $\mathbf{w}_\alpha^{(\boldsymbol{\beta})}$ and $\mathbf{w}_\alpha^{(\mathbf{H})}$ for $\alpha \to \infty$. Standard behaviour of the Tikhonov regularization yields

$$\left|\left|\mathbf{w}_\alpha^{(\mathbf{H})}\right|\right| = O\left(\frac{1}{\alpha}\right), \quad \alpha \to \infty. \tag{5.47}$$

The same holds for $\boldsymbol{\beta}_\alpha^{(\omega)}$, from which by using (5.44) we obtain

$$\mathbf{S}_{\xi,\alpha}^{(\boldsymbol{\beta})} = O\left(\frac{1}{\alpha^2}\right), \tag{5.48}$$

such that for (5.46) we obtain

$$\mathbf{w}_\alpha^{(\beta)} \sim \alpha, \quad \alpha \to \infty. \tag{5.49}$$

Since both terms depend analytically on α on $\mathbb{R}^+$, we conclude that they cannot be equal on any open subset of $\mathbb{R}^+$, which ends the proof. □

5.3. Numerical Examples

We complete our investigation by some numerical examples which demonstrate the ill-posedness of the discrimination problem in the image space under the compact operator W for the case of magnetic tomography and also show that regularized classification leads to satisfactory results. From Section 3 we have the discretized problem

$$\mathbf{WJ} = \mathbf{H} \tag{5.50}$$

to solve with a discrete Biot-Savart operator $\mathbf{W}$, the measurements $\mathbf{H} \in \mathbb{R}^M$ and the unknown currents $\mathbf{J} \in \mathbb{R}^K$. Often, we use a special basis of currents to define the matrix $\mathbf{F} = \left\{\mathbf{J}^{(1)}, ..., \mathbf{J}^{(L)}\right\} \in \mathbb{R}^{K\times L}$ and employ

$$\mathbf{WF}\boldsymbol{\beta} = \mathbf{H}, \tag{5.51}$$

where $\boldsymbol{\beta} \in \mathbb{R}^L$ is a vector of basis function coefficients. The $\mathbf{J}^{(\ell)}$ might be chosen to represent the current flowing through some particular subset of the fuel cell membrane, such that β_ℓ provides information about the quality of the particular part of the membrane, compare [13]. For all simulations the *finite integration technique* as introduced in Section 3 has been employed.

Now, the quality of fuel cells can be judged by the size of β_ℓ for $\ell = 1, ..., L$. If the homogeneous distribution is given by $\beta_\ell = c > 0$ for all ℓ, then a good cell would have β_ℓ close to c and bad cells would have β_ℓ significantly smaller than c for some $\ell \in \{1, ..., L\}$. We might choose a threshold parameter $\rho_\ell < c$ to distinguish classes C_ℓ where

$$\beta_\ell \geq \rho \quad \text{or} \quad \beta_\ell < \rho. \tag{5.52}$$

This corresponds to the classes introduced in (4.5) on a particular level L of detail. Further, physical constraints lead to $\beta_\ell \geq 0$.

For training we choose the vectors $\boldsymbol{\beta}^{(\omega)} = \left(\beta_1^{(\omega)}, ...\beta_L^{(\omega)}\right)$ of basis function coefficients randomly, so that their entries lie in the interval $[0, 1]$, where we assume $0 < c < 1$ for the

homogeneous situation described above. Then, for training the classification is achieved testing $\beta_\ell^{(\omega)} \geq \rho_\ell$, leading to $t^{(\omega)} = 1$ or $t^{(\omega)} = 0$.

Here, we will focus on using Fisher's linear discriminant applied to one of the classes C_ℓ for fixed ℓ and its complement. The calculations of the nonlinear classes (4.6) is then straightforward by taking appropriate intersections, which are achieved logically by multiplication of the corresponding target values $t_\ell^{(\omega)}$. Figure 4 shows the projected values $y^{(\omega)}$ for the case that we use vectors $\boldsymbol{\beta}^{(\omega)}$ of basis function coefficients as input vectors. Projections of input vectors with $t^{(\omega)} = 1$, i.e. belonging to class 1, have been shown as small red spheres and projections with $t^{(\omega)} = 0$, i.e. belonging to the complementary class 2, have been shown as large blue spheres. The small purple sphere is some new input vector to be classified. When its magnetic field $\mathbf{H}$ is given, we first solve (5.51) to calculate an approximation $\boldsymbol{\beta}_\alpha$ to the coefficients by Tikhonov regularization. Then, we classify $\boldsymbol{\beta}_\alpha$ via (5.1). For the values shown in Figure 4 the target values were defined using the first entry of the input vectors, i.e. $\ell = 1$. The training set size, N, is 50.

Fisher's Linear Classification on H. To perform classification using magnetic field vectors we start with random coefficients $\boldsymbol{\beta}^{(\omega)}$ as above. Then, for every vector $\boldsymbol{\beta}^{(\omega)}$ we calculate corresponding magnetic field vectors $\mathbf{H}^{(\omega)}$. The training set is

$$\left\{\left(\mathbf{H}^{(1)}, t^{(1)}\right), \cdots, \left(\mathbf{H}^{(N)}, t^{(N)}\right)\right\}, \tag{5.53}$$

where $\mathbf{H}^{(\omega)}$ are simulated values of magnetic field measurements and $t^{(\omega)}$ are the corresponding target values for $\omega = 1, \ldots, N$.

As in the previous part, we use (5.52) to define our target values. As described in (5.41) we need to use regularization techniques to calculate an approximate inverse of the within-class scatter matrix $\mathbf{S}_F^{(\mathbf{H})}$. Now, Fisher's linear discriminant is set-up by calculation of (5.42). The projection for some measured magnetic field $\mathbf{H}$ is calculated by

$$y = \left(\mathbf{w}_\alpha^{(\mathbf{H})}\right)^T \mathbf{H}. \tag{5.54}$$

Figure 5 shows results of this process for the choice $\ell = 1$. As for the corresponding classification on $\boldsymbol{\beta}$, the projections of input vectors with $t^{(\omega)} = 1$, i.e. belonging to class 1, have been shown as small red spheres and the projections with $t^{(\omega)} = 0$, i.e. belonging to the complementary class 2, have been shown as large blue spheres. The small purple sphere is some new input vector projected by (5.54), which is to be classified.

Finally, we illustrate the ill-posedness by visualization of the within-class scatter matrix $\mathbf{S}_F^{(\mathbf{H})}$ in Figure 7. The corresponding matrix $\mathbf{S}_F^{(\boldsymbol{\beta})}$ is shown in Figure 6. In the case of $\boldsymbol{\beta}$ we can see that the covariance matrix is diagonally dominant, which we expect since it is the covariance matrix of vectors with mutually independent entries. This is no longer the case for the within-class covariance matrix of the magnetic fields.

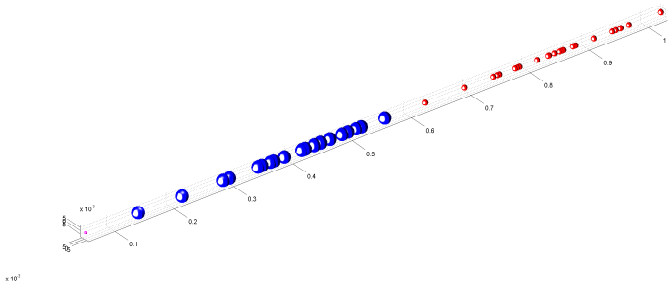

Figure 4. Fisher's linear discriminant was performed on vectors $\boldsymbol{\beta}^{(\omega)}$ of basis function coefficients, with a classification based on (5.52) for some fixed $\ell \in \{1, ..., L\}$ (with $\ell = 1$ for the particular example). Here, we show the projected values $y^{(\omega)}$ as small red spheres for $t^{(\omega)} = 1$ and large blue spheres for $t^{(\omega)} = 0$. The small purple sphere indicates a test vector which is to be classified via Fisher's linear discriminant.

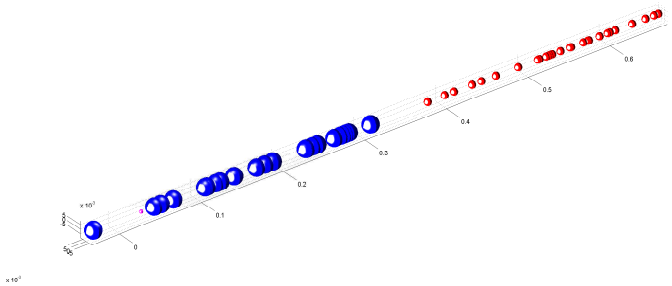

Figure 5. Regularized Fisher's linear discriminant was performed on vectors $\mathbf{H}^{(\omega)}$ of basis function coefficients, with a classification based on (5.52) for some fixed $\ell \in \{1, ..., L\}$ (with $\ell = 1$ for the particular example). As in Figure 4 we show the projected values $y^{(\omega)}$ as small red spheres for $t^{(\omega)} = 1$ and large blue spheres for $t^{(\omega)} = 0$. Again, the small purple sphere indicates a test vector which is to be classified via Fisher's linear discriminant.

References

[1] E. Andries, T. Hagstrom, S. R. Atlas, and C. Willman. Regularization strategies for hyperplane classifiers: application to cancer classification with gene expression data. *journal of bioinformatics and computational biolody*, 5:79–104, 2007.

[2] C. Bishop. *Pattern Rocognition and Machine Learning*. Springer, 2006.

[3] L. Carrette, K. A. Friedrich, and U. Stimming. Fuel cells: principles, types, fuels and applications. *A European journal of chemical physics and physical chemistry*, 1:162–193, 2001.

[4] U. Castellani, M. Cristani, A. Daducci, P. Farace, P. Marzola, and V. Murino. DCE-MRI data analysis for cancer area classification. *Methods of information in medicine*, 48:248–253, 2009.

[5] M. Chi and L. Bruzzone. An ensemble-driven k-nn approach to ill-posed classification problems.

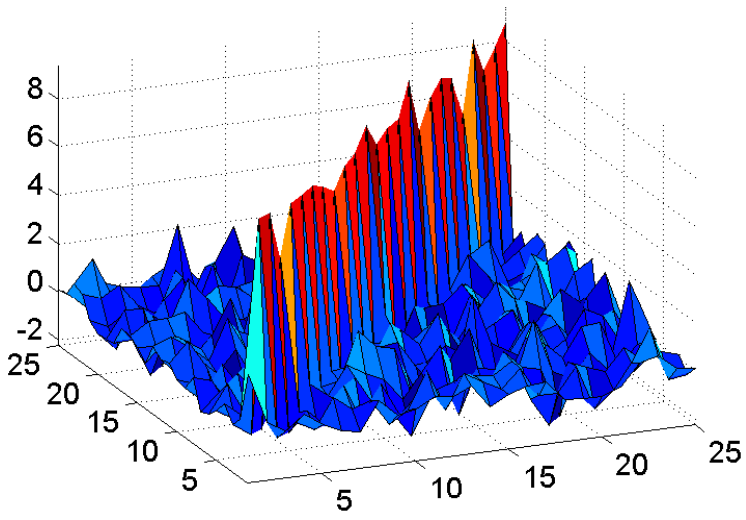

Figure 6. We visualize the entries of the within-class scatter matrix $\mathbf{S}_F^{(\boldsymbol{\beta})}$ by a surface plot.

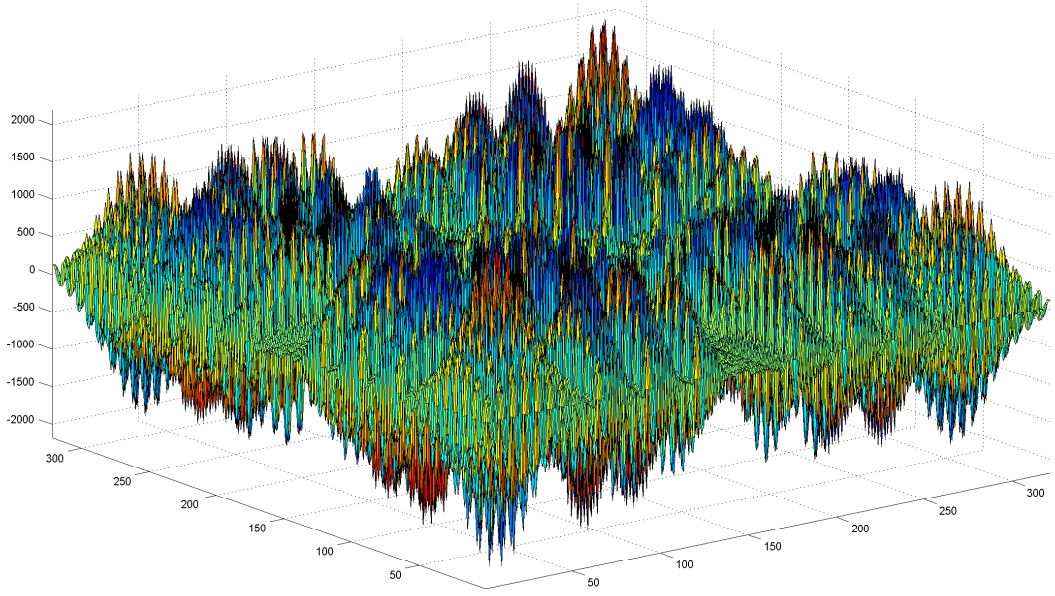

Figure 7. Three dimensional plot of entries of within-class scatter matrix, $\mathbf{S}_F$, for the case that the input vectors are magnetic field vectors. Here we have plotted every third entry of the matrix so that the figure is more clear.

pattern recognition letters, 27:301–307, 2006.

[6] D. Colton and R. Kress. *Inverse Acoustic and Electromagnetic Scattering Theory*. Springer-Verlag New York, Inc., 1998.

[7] S. Dudoit, J. Fridlyand, and P. Speed. comparison of discrimination methods for the classification of tumors using gene expression data. *journal of the American statistical association*, 97:77–87, 2002.

[8] H. Engl, M. Hanke, and A. Neubauer. *Regularization of Inverse Problems*. Kluwer Acedemic Publishers, 2000.

[9] K. Fukunaga. *Introduction to Statistical Pattern Recognition*. Academic Press, 1990.

[10] S. Gong, S. McKenna, and A. Psarrou. *Dynamic Vision: From images to Face Recognition*. Imperial College Press, 2000.

[11] K. H. Hauer, L. Kühn, and R. Potthast. On uniqueness and non-uniqueness for current reconstruction from magnetic fields. *Inverse Problems*, 21:955–967, 2005.

[12] K. H. Hauer and R. Potthast. Magnetic tomography for fuel cells - current status and problems. *Journal of Physics*, 73, 2007. 10.1088/1742-6596/73/1/012008.

[13] K. H. Hauer, R. Potthast, and M. Wannert. Algorithms for magnetic tomography - on the role of a priori knowledge and constraints. *Inverse Problems*, 24, 2008. 10.1088/0266-5611/24/4/045008.

[14] K. H. Hauer, R. Potthast, T. Wüster, and D. Stolten. Magnetomography - a new method for analysing fuel cell performance and quality. *Journal of Power Sources*, 143:67–74, 2005.

[15] A. Kirsch. *An Introduction to the Mathematical Theory of Inverse Problems*. Springer, 1996.

[16] R. Kress. *Linear Integral Equations*. Springer-Verlag New York, Inc., 1999.

[17] L. Kühn, R. Kress, and R. Potthast. The reconstruction of a current distribution from its magnetic fields. *Inverse Problems*, 18:1127–1146, 2002.

[18] H. Lustfeld, M. Reissel, and B. Steffen. Magnetotomography and electric currents in a fuel cell. *Fuel cells*, 9:474–481, 2009.

[19] T. Poggio, V. Torre, and C. Koch. Review article: Computational vision and regularization. *Nature*, 317:314–319, 1985.

[20] Potthast. *Point Sources and Multipoles in Inverse Scattering Theory*. Chapman & Hall, 2001.

[21] R. Potthast and L. Kühn. On the convergence of the finite integration technique for the anisotropic boundary value problem of magnetic tomography. *Mathematical Methods in the Applied Sciences*, 26:739–757, 2003.

[22] R. Potthast and M. Wannert. Uniqueness of current reconstructions for magnetic tomography in multilayer devices. *SIAM Journal on Applied Mathematics*, 70:563–578, 2009.